Anchored and labile pools of Calcineurin are enabled by a disordered AKAP scaffold

Authors

Matthew Watson[a], Teresa B. Almeida[a], Arundhati Ray[a], Christina Hanack[b], Rory Elston[a], Joan Btesh[b], Peter A. McNaughton[c] & Katherine Stott[a,*]

[a]Department of Biochemistry, University of Cambridge, 80 Tennis Court Road, Cambridge CB2 1GA, UK

[b]Stevenage Bioscience Catalyst, Gunnels Wood Rd, Stevenage SG1 2FX

[c]Wolfson Centre for Age-Related Diseases, King's College London, Guy's Campus, London Bridge, London, SE1 1UL, UK

[*]To whom correspondence should be addressed: ks123@cam.ac.uk

Present addresses:

TA: Astex Therapeutics, 436 Cambridge Science Park, Milton Road, Cambridge, CB4 0QA, UK

AR: School of Life Sciences, Gibbet Hill Campus, The University of Warwick, Coventry CV4 7AL

CH: Axxam SpA, Via Meucci 3, 20091 Bresso (Milan, Italy)

RE: Department of Biology, University of York, Heslington, York, YO10 5DD, UK

ORCIDs:

PM: 0000-0003-1946-9610

KS: 0000-0002-4014-1188

Keywords: intrinsically disordered protein, A-kinase anchoring protein (AKAP), Calcineurin, short linear motif (SLiM), multivalency, allovalency

Abstract

Signalling requires precise spatial and temporal regulation of molecular interactions, which is frequently orchestrated by disordered scaffolding proteins, such as A-kinase anchoring protein 5 (AKAP5). AKAP5 contains multiple Short Linear Motifs (SLiMs) that assemble the necessary components, including the phosphatase Calcineurin, which is anchored *via* a well-characterised PxIxIT SLiM. Here we show, using a combination of biochemical and biophysical approaches, that Calcineurin also recognises additional lower-affinity SLiMs C-terminal to the PxIxIT motif. Moreover, we demonstrate that the assembly is in reality a complex system in which AKAP SLiMs spanning a wide affinity range act cooperatively to maintain distinct pools of anchored and more loosely held enzyme, analogous to transcription factor search complexes on DNA, and compatible with the requirement for both stable anchoring and responsive downstream signalling. We conclude that the AKAP5 C-terminus is enriched in lower-affinity/mini-SLiMs that cooperate to maintain a structurally disordered but tightly regulated signalosome.

Introduction

Many enzymes involved in signal transduction are promiscuous and act in multiple pathways. Scaffolding proteins are therefore central to signalling since, by tethering signalling components and localising them, they enhance specificity and reaction rates by effectively enhancing local concentrations, and thereby achieve strict spatial and temporal control of catalysis (1, 2). A-kinase anchoring proteins (AKAPs) are a family of intrinsically-disordered proteins (IDPs) that were originally characterized by their ability to scaffold Protein Kinase A (PKA) (3, 4), but have since been shown to assemble multiple components into 'signalosomes' that can be targeted to specific receptors or sites (5, 6). Currently there are 14 annotated AKAPs in humans (AKAP1 to AKAP14).

AKAPs are typical of many IDPs in that they interact with their partners *via* Short Linear Motifs (SLiMs) (7, 8). The presence of multiple SLiMs with different specificities in AKAPs enables the combinatorial assembly of a dynamic multi-protein hub. Much of what we understand about disordered signalling complexes is based on the structures of folded partners bound to their peptide SLiMs. The rest of the IDP is either not resolved or is removed to facilitate structural studies. In many cases, the regions between SLiMs are assumed to be inert linkers, simply providing a length-dependent increase in the effective concentration, although predictions from physical models are not always reproduced experimentally, suggesting the reality is more complicated (9). The context in which IDP(R) partner interactions take place can also play an important role (10). The flanking sequences around SLiMs, although disordered even in the complex, often contribute to binding (11). Moreover, there can be complex interplay between SLiMs (7). For example, clustering or overlapping SLiMs can modulate interactions through cooperativity or competition. Further, multiple low-affinity SLiMs binding a single target can cooperate in a multivalent interaction to increase the binding affinity. The cooperativity can take different forms: e.g. allovalency (where multiple epitopes along the ligand bind a single site on

75 a partner (12)), or 'fuzziness' (where multiple interchangeable interaction sites exist
76 on both the ligand and partner (13)).
77 Here we study the interaction of the ubiquitous phosphatase Calcineurin
78 (also known as PP2B) with the C-terminal region of the scaffolding protein AKAP5
79 (previously known as AKAP79 in humans and AKAP150 in mice). Calcineurin couples
80 changes in intracellular calcium concentration to the phosphorylation state of
81 several important substrates (14). One example is the NFAT (Nuclear Factor of
82 Activated T cells) family of transcription factors, which are dephosphorylated by
83 Calcineurin, causing their translocation to the nucleus and stimulation of
84 transcriptional programmes (15). Like other phosphatases, Calcineurin
85 dephosphorylates sites with little sequence similarity (16, 17), and primarily
86 recognises substrates or their scaffolding proteins through the interaction with
87 SLiMs, such as the PRIEIT sequence in NFATc1 (18, 19). PRIEIT is a canonical
88 Calcineurin recognition motif obeying the consensus sequence PxIxIT, a so-called
89 'PxIxIT' SLiM. This interaction has a 25 µM affinity, which is within the optimal
90 window for its signalling function (20). AKAP5 also has a PxIxIT SLiM with which it
91 engages Calcineurin, albeit one with a higher affinity – PIAIIIT – that is suited to
92 anchoring (0.4 µM), while not so tight that downstream signalling is inhibited (21). In
93 this study, we examined the AKAP5/Calcineurin interaction from the perspective of
94 the IDP scaffold. Using Surface Plasmon Resonance (SPR) and NMR spectroscopy, we
95 show that binding is far more extensive than the PxIxIT alone and we identify
96 additional regions that interact with µM - mM affinity. We hypothesise that these
97 additional low-affinity sites help to capture and maintain the high-affinity anchored
98 Calcineurin. Moreover, they provide a separate 'labile but localised' pool of rapidly
99 dissociating and rebinding Calcineurin, which could be intercepted by proteins such
100 as NFAT that compete for Calcineurin in order to enact optimal downstream
101 signalling.
102
103

Results

The AKAP5c scaffold is highly disordered and monomeric

AKAP5 can loosely be divided into three regions (Fig. 1a). Here, we have chosen to focus on the C-terminal region (300-427; AKAP5c), which we define as the region of homology across various species (Supp. Fig. S1) following a large insertion of unknown function in the rodent orthologues. The sequence contains three known SLiMs that bind either enzymes (Calcineurin (22, 23) or PKA (24)) or substrates (TRPV1/4 (25–27)). The enzyme-bound SLiMs adopt defined secondary structures in

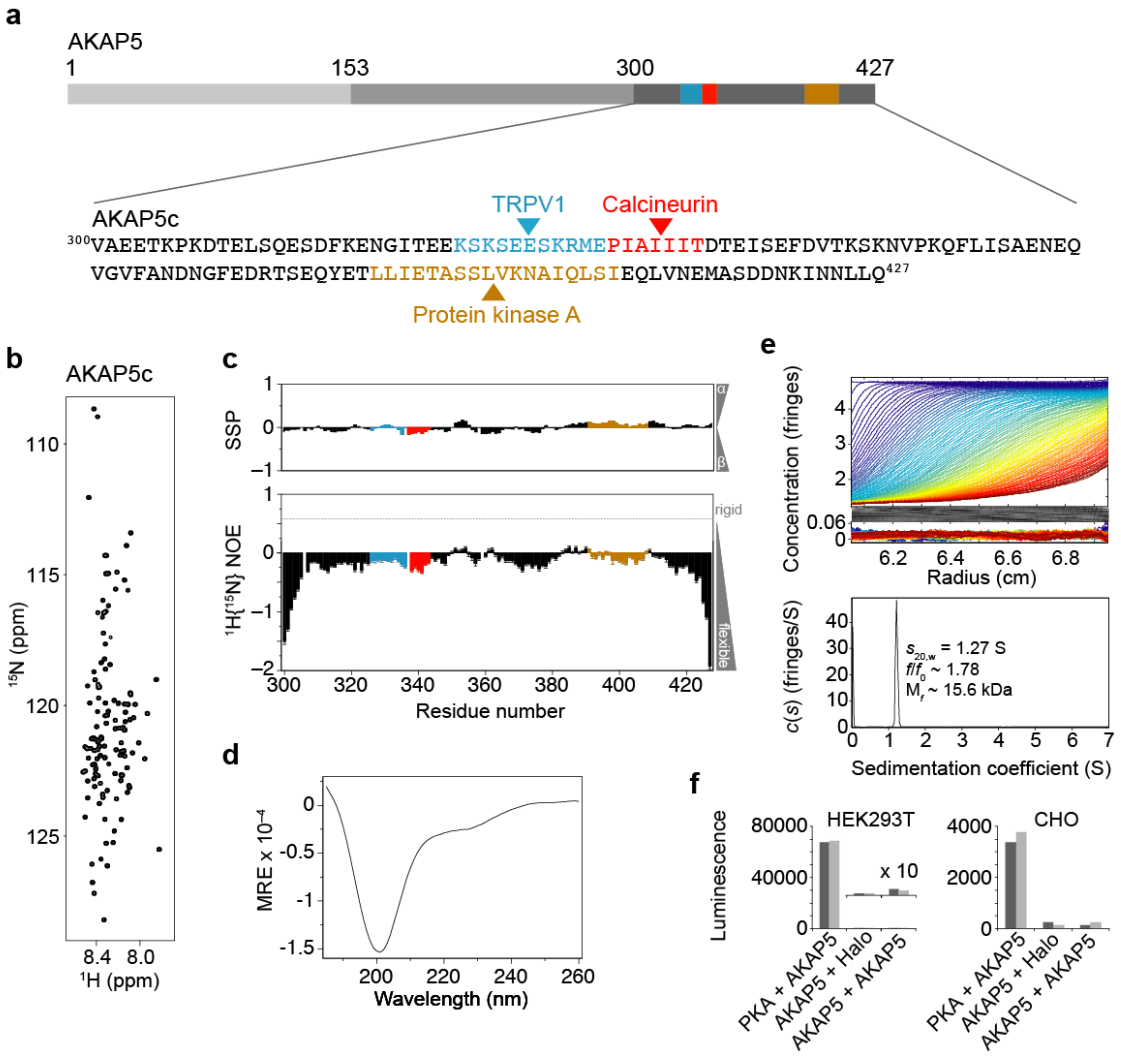

Figure 1: Structure, hydrodynamic properties and oligomeric state of AKAP5$_{300\text{-}427}$ (AKAP5c). (**a**) Schematic of AKAP5: the N-terminal region (1-153) is involved in membrane attachment; the middle region (154-299) is recognised by scaffolding proteins of the Membrane associated Guanylate Kinase family; and the C-terminal region (300-427, shown expanded) contains three known SLiMs that bind Calcineurin, PKA and substrates e.g. TRPV1. (**b**) ^{15}N HSQC of AKAP5c. (**c**) Secondary structure propensity (SSP) and Heteronuclear NOE values (colouring of SLiMs as **a**). (**d**) Far-UV CD spectrum. (**e**) Sedimentation velocity continuous *c*(*s*) distribution. (**f**) Live HEK- and CHO-cell split-luciferase assays (NanoBiT®, Promega). AKAP5 = full-length protein, PKA = regulatory PKA subunit (R2A) (positive control), Halo = HaloTag® (negative control). The order of listing indicates the orientation of the split luciferase: <protein>-LgBiT + <protein>-SmBiT.

112 the complexes: a β-strand in the case of Calcineurin (21) and an α-helix in the case of
113 the docking and dimerization (D/D) domain of PKA (24). There is no structural
114 information on the SLiM reported to bind TRPV1/4 (25, 26).
115 To fully understand the role of disorder in the assembly of signalling
116 complexes by scaffolding proteins, it is important to understand the level and type of
117 disorder present. The term "intrinsic disorder" (28) is used to describe all proteins
118 that populate transient structures through to those that approach true random coils
119 (i.e. those with no structural preferences and uniformly fast backbone dynamics).
120 Two spectroscopic techniques were deployed to assess and delineate regions of
121 nascent structure and to probe the backbone dynamics in AKAP5c: nuclear magnetic
122 resonance (NMR) and circular dichroism (CD). The ^{15}N-HSQC spectrum (Fig. 1b)
123 displays the low $^{1}H^{N}$ chemical-shift dispersion (0.7 ppm) and narrow line widths
124 typical of disordered proteins. A near complete assignment of the backbone H, C, N
125 and C^{β} chemical shifts was possible (Supp. Fig. S2), from which the secondary
126 structure propensity (SSP (29)) could be calculated (Fig. 1c). SSP scores in AKAP5c are
127 close to zero with alternating stretches of weak α- or β-propensities. For
128 comparison, SSP scores are ca. +1 or –1 in stable α- and β-structures, respectively. It
129 is interesting to note that the propensities of the Calcineurin- and PKA-binding SLiMs
130 (red and yellow, respectively, in Fig. 1c) reflect the stable structures adopted in the
131 bound states (SSP_{mean} = –0.116 ± 0.038 and +0.079 ± 0.037, i.e. weak β and α,
132 respectively). Backbone dynamics were probed by $\{^{1}H\}^{15}N$ heteronuclear NOE
133 (HNOE; Fig. 1c), which reveals motions on a time-scale faster than overall tumbling
134 (HNOE < ca. +0.6). HNOEs were fairly uniform throughout AKAP5c (disregarding the
135 highly mobile N- and C-termini). The average value was –0.20 ± 0.29, with no single
136 residue exhibiting a value > +0.1, and all SLiMs falling within one standard deviation
137 of the mean. This is consistent with a highly dynamic polypeptide chain. CD
138 spectroscopy also showed AKAP5c to be predominantly disordered (Fig. 1d): the
139 signature large negative ellipticity at 200 nm was dominant, although there were

140 indications of some secondary structure (as evidenced by the weak shoulder at 222
141 nm) that is likely to be transiently populated given the results from NMR.
142 We next investigated the hydrodynamic properties of AKAP5c by
143 sedimentation velocity analytical ultracentrifugation (SV AUC, Fig. 1e). AKAP5c
144 sedimented slowly ($s_{20,w}$ = 1.27) due to hydrodynamic friction resulting from its
145 extended nature (frictional ratio f/f_0 ~ 1.78). The fitted mass (~ 15.6 kDa) was close
146 to the calculated monomer mass (14.5 kDa). The overall picture of AKAP5c is
147 therefore one of a highly dynamic and monomeric chain. However, there are reports
148 that AKAP5 can dimerise (30, 31). Of particular relevance to this study is the
149 observation of K333-K333 and K328-K328 intermolecular crosslinks (30), which are in
150 the TRPV1/4 interaction SLiM immediately N-terminal to the Calcineurin binding site.
151 Conversely, Nygren *et al*. (32) concluded that the AKAP5/Calcineurin complex is
152 monomeric by SEC-MALS. Calcineurin is a heterodimer of A and B subunits, which
153 are not reported to oligomerise further (14), although we observed a weak
154 propensity for further dimerisation by SV AUC (Supp. Fig. S3).
155 Given AKAP5 forms complex assemblies within the cell, we investigated
156 whether full length AKAP5 dimerises in a cellular context (HEK293T and CHO) with a
157 highly sensitive live-cell luminescence assay (NanoBiT®, Promega) that uses a split-
158 luciferase reporter engineered to give reduced background. A strong
159 complementation signal was seen between PKA and AKAP5, however, AKAP5 did not
160 give a self-complementation signal in these assays that was significantly different
161 from the HaloTag® negative control (Fig. 1f). This does not preclude AKAP chains
162 being brought into spatial proximity *in vivo* by interactions with multimeric
163 receptors, e.g. tetrameric TRPV1 (33).
164
165
166
167
168

169 **Calcineurin binding extends beyond the PxIxIT site**

170 The Calcineurin anchoring site in AKAP5c is at ^{337}PIAIIIT^{343}, a near-consensus PxIxIT
171 SLiM (18, 19), in which ^{338}I takes the position of the consensus proline. In the crystal
172 structure, ^{337}P is not engaged and van der Waals contacts extend ca. five residues C-
173 terminal of the PxIxIT site (21). To investigate the involvement of more distal flanking
174 regions, we titrated Calcineurin into ^{15}N-labelled AKAP5c and followed binding by ^{15}N
175 HSQC (Fig. 2a). After one molar equivalent of Calcineurin had been added, many
176 peaks had decreased significantly in intensity, including those from residues
177 ^{338}IAIIIT^{343} (shown boxed), although the intensity loss was not complete. The changes
178 were purely to the peak intensities; no significant chemical-shift changes were seen,
179 nor did the peaks get broader, indicating that the interaction was slow on the
180 chemical-exchange timescale. No new peaks appeared, indicating slow overall
181 tumbling of the complex (Calcineurin is 80 kDa), rendering the residues in the region
182 engaging with Calcineurin invisible. The relative intensity changes when mapped
183 onto the sequence extend approx. 24 residues C-terminal beyond the PIAIIIT site,
184 with further broad dips around residues 390 and 410 (Fig. 2b). Calcineurin binding
185 thus not only extends well beyond the PIAIIIT SLiM (which could be due to weak and
186 transient interactions extending the footprint) but also involves distal regions of the
187 C-terminus of AKAP5c.

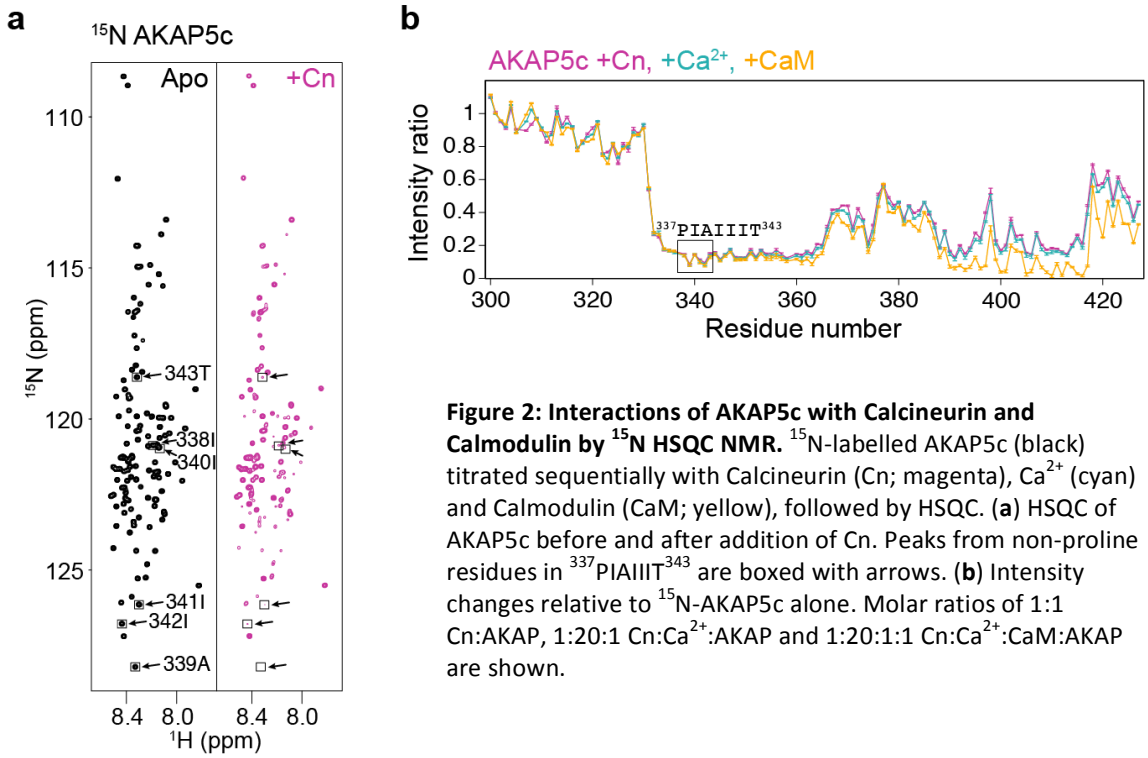

Figure 2: Interactions of AKAP5c with Calcineurin and Calmodulin by ^{15}N HSQC NMR. ^{15}N-labelled AKAP5c (black) titrated sequentially with Calcineurin (Cn; magenta), Ca^{2+} (cyan) and Calmodulin (CaM; yellow), followed by HSQC. (**a**) HSQC of AKAP5c before and after addition of Cn. Peaks from non-proline residues in ^{337}PIAIIIT^{343} are boxed with arrows. (**b**) Intensity changes relative to ^{15}N-AKAP5c alone. Molar ratios of 1:1 Cn:AKAP, 1:20:1 Cn:Ca^{2+}:AKAP and 1:20:1:1 Cn:Ca^{2+}:CaM:AKAP are shown.

188 **Calcium and Calmodulin do not significantly alter binding**

189 Calcineurin has a regulatory domain that renders it enzymatically dormant in the
190 absence of Ca^{2+} and Calmodulin. Increases in Ca^{2+} concentration lead to partial
191 activation of Calcineurin, through loosening association of the regulatory domain
192 and exposure of the Calmodulin binding region. Further binding of Ca^{2+}-Calmodulin
193 results in full activation (15, 34). In addition to stimulating Calcineurin activity, this
194 exposes a second SLiM-binding region, that interacts with binding partners
195 containing a πϕLxVP motif (π = polar, ϕ = hydrophobic) in a Ca^{2+}-Calmodulin
196 dependent manner (35). Although the focus of this study is on the dormant complex
197 in which the πϕLxVP binding pocket in Calcineurin is occluded by the regulatory
198 domain, we wanted to establish whether Ca^{2+} or Ca^{2+}-Calmodulin binding alters the
199 interaction with PIAIIIT or the new interactions found above.

200 We first titrated the pre-formed AKAP/Calcineurin 1:1 complex with Ca^{2+},
201 followed by Calmodulin. No changes were seen on addition of Ca^{2+} to a large excess
202 (20:1; Fig. 2b). AKAP5c/Calcineurin binding is therefore calcium-independent. On
203 addition of Calmodulin to 1:1:1 Calmodulin:Calcineurin:AKAP in excess Ca^{2+}, no
204 changes were seen in the region of PIAIIIT, indicating that PIAIIIT-binding of
205 Calcineurin was unaffected, in line with pull-down experiments from other
206 laboratories (30, 32). However, further peak attenuation was observed in the region
207 C-terminal but distal to the PIAIIIT site, spanning residues 390-417 (Fig. 2b). In this
208 case, peaks visibly broadened and shifted, indicating intermediate-to-fast exchange
209 on the chemical shift time scale (unlike for Calcineurin binding, in which the peaks
210 disappeared), suggesting that Calmodulin binds to the same site. Consistent with
211 this, a separate titration of AKAP with Ca^{2+} and Calmodulin alone showed larger
212 chemical shift changes for the same peaks along the same trajectories, indicating a
213 larger mole fraction of CaM bound in the absence of Calcineurin (Supp. Fig. S4).
214 Calmodulin therefore appears to compete with Calcineurin for binding to residues
215 390-417, a region ca. 50 residues from the canonical PxIxIT site. This region is known
216 to form an amphipathic helix on binding PKA, and contains two clusters of bulky

217 hydrophobic residues separated by a stretch of polar residues, which is a feature of
218 Calmodulin binding (36), although the sequence was not predicted to be Calmodulin-
219 binding by a database search (Calmodulin Target Database
220 (http://calcium.uhnres.utoron- to.ca/ctdb/)). We could not confirm whether
221 Calmodulin also bound Calcineurin in the canonical manner, but the pattern of
222 shifting and broadening of peaks continued beyond a 1:1 molar ratio of Calmodulin,
223 which is compatible with binding to two sites.
224

225 **PxIxIT is not required for binding to non-canonical sites**

226 Given the involvement of PxIxIT-flanking and distal regions of AKAP5c in binding to
227 Calcineurin, we investigated binding to AKAP5c in which the PIAIIIT site had been
228 deleted, AKAP5c$_{\Delta PIAIIIT}$. The titration with Calcineurin (Fig. 3a) was carried out as
229 previously. From the overlay of the intensity ratios (Fig. 3b), it is clear that the

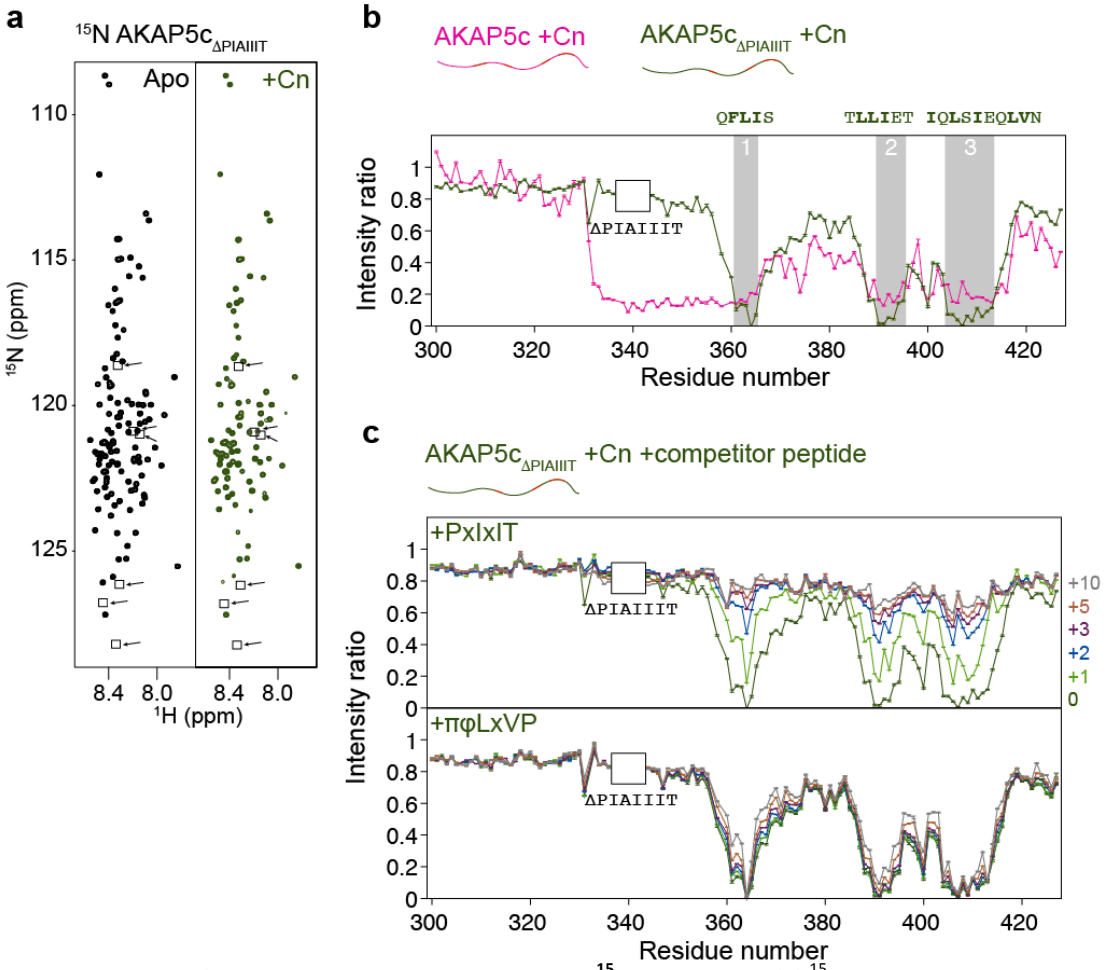

Figure 3: Interactions of AKAP5c$_{\Delta PIAIIIT}$ with Calcineurin by ^{15}N HSQC NMR. (**a**) ^{15}N-labelled AKAP5c$_{\Delta PIAIIIT}$ alone (black; positions of deleted ^{337}PIAIIIT^{343} residues shown boxed with arrows). AKAP5c$_{\Delta PIAIIIT}$ titrated with Calcineurin (Cn) to 1:1 Cn:AKAP (green). (**b**) Intensity changes relative to ^{15}N-AKAP5c$_{\Delta PIAIIIT}$ alone. Corresponding WT data (magenta) reproduced from Fig. **2b**. Grey boxed regions 1-3 indicate Cn binding sites in AKAP5c$_{\Delta PIAIIIT}$, with the corresponding amino acid sequences shown above. (**c**) Titrations of the 1:1 AKAP5c$_{\Delta PIAIIIT}$:Cn complex with PxIxIT and πφLxVP peptides (0 to 10 molar equivalents shown).

230 immediate footprint around the PIAIIIT site (residues 330-350) is lost, as expected.
231 However, intensities more distal to the PIAIIIT site still showed significant decreases
232 in intensity, in the same regions and even more pronounced than in WT AKAP5c.
233 Three regions with pronounced dips in intensity were seen, ^{361}QFLIS^{365}, ^{390}TLLIET^{395}
234 and ^{404}IQLSIEQLVN^{413}, which we termed secondary sites 1, 2 and 3, respectively.
235 Binding to these sites therefore does not depend on the presence of the
236 PIAIIIT site. Moreover, there is some evidence for competition with PIAIIIT since
237 deletion of PIAIIIT appears to enhance binding to secondary sites. An important
238 question not resolved by these experiments is whether PIAIIIT and the secondary
239 sites bind to the same or different sites on Calcineurin. In order to address this, the
240 1:1 ^{15}N-AKAP5c$_{\Delta PIAIIIT}$/Calcineurin complex was further titrated with a PIAIIIT-
241 containing peptide (EPIAIIITDTE; Fig. 3c). The peptide proved an effective
242 competitor; ^{15}N-AKAP5c$_{\Delta PIAIIIT}$ peak intensities were almost fully restored after
243 addition of three molar equivalents of the peptide (Fig. 3c, top). Given the similar
244 hydrophobicity of the secondary sites to the πϕLxVP motif, the experiment was
245 repeated with a πϕLxVP peptide (DDQYLAVPQH (35)), which was ineffective even
246 upon addition of ten molar equivalents (Fig 3c, bottom). The recognition site for
247 secondary sites 1, 2 and 3 is thus the PxIxIT-binding groove in Calcineurin and not the
248 πϕLxVP binding site.
249 The secondary site sequences each contain three or more bulky hydrophobic
250 residues and include isoleucine, which together are likely to underpin binding to the
251 PxIxIT-binding groove. Therefore, a further AKAP mutant was tested: AKAP$_{ILVF\text{->}SA}$, in
252 which the PIAIIIT site was present, but all the hydrophobic I, L, V and F residues in
253 the three secondary sites were mutated to S or A to give ^{361}QASAS^{365}, ^{390}TASAET^{395}
254 and ^{404}AQSSAEQSAN^{413}. Following reassignment of the chemical shifts, the protein
255 was again titrated with Calcineurin (Fig. 4a). Similar to the WT, large reductions in
256 intensities were observed in and around the PIAIIIT site (Fig. 4b). This was more
257 pronounced in AKAP$_{ILVF\text{->}SA}$ indicating higher occupancy of the site by Calcineurin,
258 consistent with removal of competing secondary sites. No dips were seen at

259 secondary sites 2 and 3, (intensities were similar to the unbound AKAP) and site 1
260 was partially attenuated (overlap with the PxIxIT footprint made the effect less
261 clear). The secondary sites therefore each constitute additional hydrophobic SLiMs
262 that despite not being canonical PxIxIT sites, are nevertheless recognised by the
263 PxIxIT-binding pocket on Calcineurin. One small extra region of non-PIAIIIT
264 interaction was apparent in $AKAP_{ILVF->SA}$ in the absence of the secondary sites:
265 ^{371}VGVFA^{375}, which contains three bulky hydrophobic residues but no isoleucine, and
266 there were also weaker dips corresponding to regions containing just one or two
267 hydrophobic residues: ^{378}NGFED^{382}, ^{386}EQYET^{390}, ^{398}SLVKN^{402} and ^{424}NLLQ^{427} (shown
268 by asterisks in Fig. 4b). We hereon refer to these as 'mini-SLiMs' in order to
269 differentiate them from the primary and secondary sites.

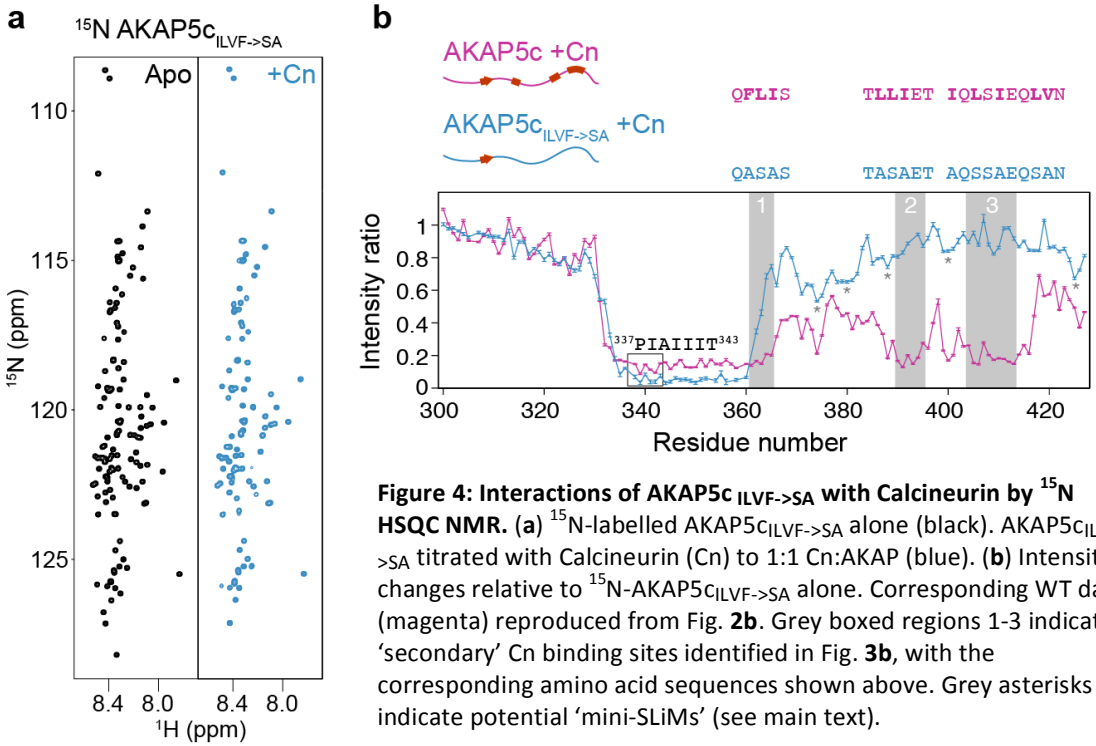

Figure 4: Interactions of AKAP5c $_{ILVF->SA}$ with Calcineurin by ^{15}N HSQC NMR. (**a**) ^{15}N-labelled $AKAP5c_{ILVF->SA}$ alone (black). $AKAP5c_{ILVF->SA}$ titrated with Calcineurin (Cn) to 1:1 Cn:AKAP (blue). (**b**) Intensity changes relative to ^{15}N-$AKAP5c_{ILVF->SA}$ alone. Corresponding WT data (magenta) reproduced from Fig. **2b**. Grey boxed regions 1-3 indicate 'secondary' Cn binding sites identified in Fig. **3b**, with the corresponding amino acid sequences shown above. Grey asterisks indicate potential 'mini-SLiMs' (see main text).

270

271 **Non-canonical sites sequester additional Calcineurin**

272 The detection of three secondary Calcineurin-binding SLiMs led us to speculate
273 about their relative affinity compared to PxIxIT, and whether there is interplay
274 between them. Modified AKAP constructs, Cys-AKAP5c, Cys-$AKAP5c_{\Delta PIAIIIT}$ and Cys-

275 AKAP5c$_{ILVF->SA}$ were chemically biotinylated for N-terminal-specific immobilisation on
276 a streptavidin surface so that Calcineurin binding could be assessed by SPR.
277 Calcineurin binding to AKAP5c (Fig. 5a) was clear but complex: the response curves
278 (1) had no clear plateau and (2) displayed evidence of multiple binding sites with
279 both fast and slow kinetics in both the association and dissociation phases. In
280 addition, a fraction of the Calcineurin remained bound at long times. The complexity
281 was reduced somewhat in the curves for AKAP5c$_{ILVF->SA}$ (Fig. 5b), which showed a
282 clear saturation plateau that was absent in the WT, and complete dissociation. For
283 AKAP5c$_{\Delta PIAIIIT}$ (Fig. 5c), the curves showed a clear plateau and complete dissociation,
284 but weaker overall binding. Also noteworthy was that the binding curves for
285 AKAP5c$_{ILVF->SA}$ and AKAP5c$_{\Delta PIAIIIT}$ did not sum to reproduce the AKAP5c binding curve,

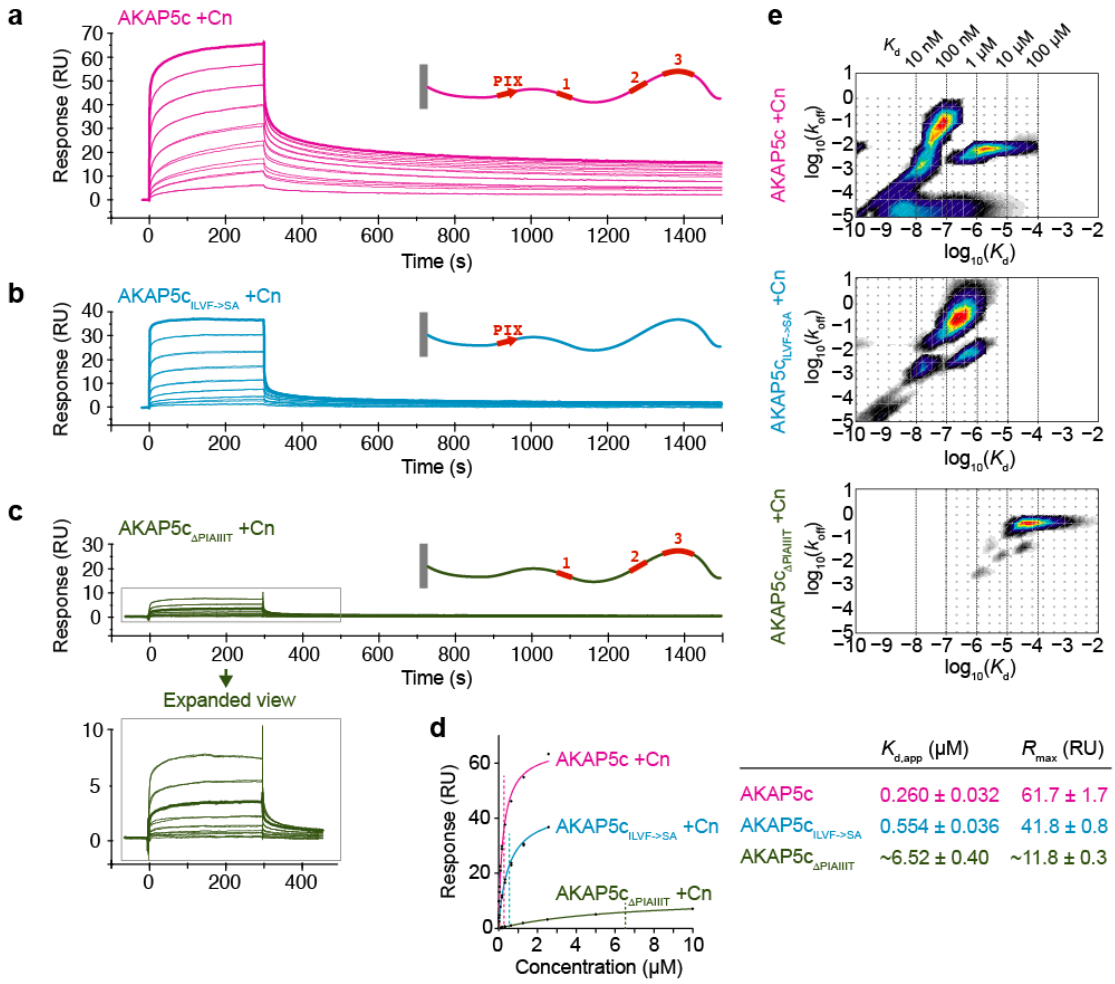

	$K_{d,app}$ (μM)	R_{max} (RU)
AKAP5c	0.260 ± 0.032	61.7 ± 1.7
AKAP5c$_{ILVF->SA}$	0.554 ± 0.036	41.8 ± 0.8
AKAP5c$_{\Delta PIAIIIT}$	~6.52 ± 0.40	~11.8 ± 0.3

Figure 5: cAKAP/Calcineurin binding by surface plasmon resonance. Calcineurin injected over a streptavidin surface pre-immobilised with (**a**) AKAP5c, (**b**) AKAP5c$_{ILVF->SA}$ or (**c**) AKAP5c$_{\Delta PIAIIIT}$. Calcineurin concentrations were 2-fold dilutions from 2.56 μM (AKAP5c and AKAP5c$_{ILVF->SA}$) or 10 μM (AKAP5c$_{\Delta PIAIIIT}$). (**d**) Fits of 'steady-state' response vs Calcineurin concentration used to obtain estimates of $K_{d,app}$ and R_{max}. (**e**) Surface site complexity modelled in Evilfit (37): distribution plots of k_{off} vs K_d obtained by fitting the data from **a**-**c** using a regularization and Bayesian approach (see Supp. Fig. S5 for further details).

286 i.e. A ≠ B + C, despite their comprising separately the two kinds of binding site
287 present in the WT. This was particularly apparent in the dissociation phase, where
288 the WT showed a sizeable fraction of Calcineurin was essentially permanently
289 bound, while no long-lasting binding of Calcineurin was observed with either mutant.
290 The binding to the PxIxIT and the secondary sites is therefore cooperative.
291 An estimate of the K_d could be obtained from fitting the signal (RU) at the
292 end of the association period *vs* Calcineurin concentration (Fig. 5d). The values
293 obtained can only be estimates for AKAP5c and AKAP5c$_{\Delta PIAIIIT}$ due to the lack of
294 saturation ('steady-state') of the former and the lack of high-concentration data for
295 the latter. Nevertheless, the trend in apparent K_d is clear: AKAP5c binds Calcineurin
296 about twice as tightly compared to AKAP5c$_{ILVF\text{->}SA}$, (K_d ~0.3 vs 0.6 µM) while both
297 PIAIIIT-containing AKAP constructs bind Calcineurin with at least ten-fold higher
298 affinity than AKAP5c$_{\Delta PIAIIIT}$, which has a K_d of ~ 10 µM. Estimation of the total surface
299 capacity for Calcineurin (R_{max}) is also instructive as it gives information on the
300 stoichiometry of binding under saturating conditions. From extrapolation of the
301 binding curves, it appears that AKAP5c can accommodate ca. 50% more Calcineurin
302 than AKAP5c$_{ILVF\text{->}SA}$ (62 vs 42 RU; Fig. 5d). The secondary sites may account for this
303 'extra' 20 RU capacity, since R_{max} for AKAP5c$_{\Delta PIAIIIT}$ is (very approximately) 12 RU.
304 Multivalent ligands such as AKAP5c are intrinsically heterogeneous, and thus
305 deviation from ideal pseudo-first order binding kinetics is not unexpected. Such
306 systems require a different analysis strategy if they are to be properly characterised.
307 A suitable alternative approach has been developed by Schuck and colleagues
308 ('Evilfit'; (37)), which uses modern regularization methods combined with a Bayesian
309 approach to add features that are essential to explain the observed data to the
310 single species model. Such features could be populations of lower-affinity or poorly
311 reversible sites. With this approach, it was possible to obtain excellent fits to the raw
312 SPR data (Supp. Fig. S5), and to extract k_{off} vs K_d distribution plots (Fig. 5e). The
313 complexity seen for Calcineurin binding to AKAP5c was deconvolved into 3 or 4
314 classes of surface sites: one or possibly two very similar sites with K_d 10-100 nM,

315 another with K_d 1-10 µM, and a final class with a very slow k_{off} that presumably
316 accounts for the lack of full dissociation observed even at long times (i.e. poor
317 reversibility). The number of surface site classes was reduced in AKAP5c$_{ILVF->SA}$ to one
318 main site with K_d 100 nM-1 µM. The distribution was simpler again for AKAP5c$_{\Delta PIAIIIT}$
319 which displayed a single class of sites with K_d 10-100 µM (the true value is likely to lie
320 at the lower end of this range given the value obtained from the equilibrium fit in
321 Fig. 5d (~10 µM) and the fact that a high fraction bound was seen by NMR at a
322 concentration of 100 µM (Fig. 3b)). These results support a picture in which AKAP5c
323 acts as a multivalent surface capable of binding one or more molecules of
324 Calcineurin at different sites. There are also strong indications that the PIAIIIT and
325 secondary binding sites bind cooperatively. Firstly, the K_d seems to vary by as much
326 as an order of magnitude dependent on the presence or absence of the other class
327 of site (Fig. 5e). For two-site binding in the absence of cooperativity, the overall
328 observed association constant will be $K = K_A + K_B$. Given the apparent overall K_ds are
329 $K_{d,WT}$ = 0.26, $K_{d,ILVF->SA}$ = 0.55 and $K_{d,\Delta PIAIIIT}$ ~10 µM (Fig. 5d), the K_as are $K_{a,WT}$ ~ 3.8,
330 $K_{a,ILVF->SA}$ ~ 1.8 and $K_{a,\Delta PIAIIIT}$ ~ 0.1 µM^{-1}. Clearly, 3.8 > 1.8 + 0.1, indicating positive
331 cooperativity. Secondly, there appears to be a 'long-lived' (slow k_{off}) bound
332 population that is only significant when both sites are present (Fig. 5a&e). This latter
333 phenomenon is reminiscent of the re-capture behaviour seen for bivalent
334 antibodies, which also show anomalously slow dissociation, or ligands rebinding to
335 receptors at cell surfaces (38).
336
337 **Discussion**
338 From our experiments, it is clear that the Calcineurin binding site in AKAP5c is far
339 more extensive than PIAIIIT, involving additional SLiMs and 'mini-SLiMs' in the C-
340 terminal region that interact with µM-mM affinity: non-consensus SLiMs containing
341 as few as three bulky hydrophobic residues appear able to bind Calcineurin with low-
342 to-mid µM affinity (AKAP5c$_{\Delta PIAIIIT}$; Fig. 5d&e), and mini-SLiMs containing only one or
343 two hydrophobic residues produce detectable binding by ^{15}N-HSQC (Fig. 4b). These

344 additional sites cooperate to increase both the effective affinity, and potentially the
345 binding capacity of the scaffold. The effective affinity is likely to be raised through
346 both an increase in the number of productive encounters given the high density of
347 SLiMs, and through rebinding mechanisms that reduce the diffusion of Calcineurin
348 away from the scaffold since the molecule is likely to be intercepted by another
349 binding site rather than diffusing away. We note that a recently developed model for
350 competitive two-site binding showed that the bound population at one site can
351 influence kinetics of binding at the other where they are connected by a diffusion
352 pathway (39). This latter point is borne out directly in our experiments by the lack of
353 complete dissociation of Calcineurin on AKAP5c seen by SPR (Fig. 5a). The 'labile but
354 localised' pool of rapidly dissociating, diffusing and rebinding Calcineurin can
355 presumably also be captured by downstream effectors such as NFAT despite their
356 mid µM affinities (Fig. 6).

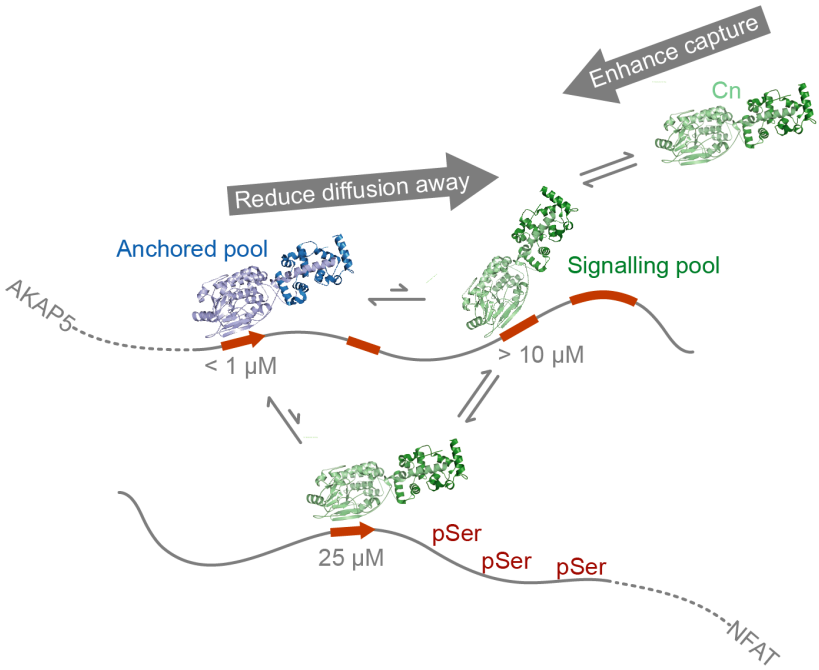

Figure 6: Non-canonical SLiMs could facilitate both anchoring and formation of a labile Calcineurin pool that enables efficient transfer to effectors. AKAP5c captures and retains Calcineurin using its consensus PIAIIIT (red arrow) and secondary sites (red rectangles), building anchored and signalling pools of bound Calcineurin (blue and green, respectively). Calcineurin binds with lower-affinity to the secondary sites, enabling effective competition by weaker PxIxIT motifs on downstream effectors, e.g. the PRIEIT SLiM in NFAT, and optimal signalling.

357 These new insights are made possible by the combination of NMR
358 experiments and a non-traditional approach to SPR data fitting that is validated by
359 strategic mutagenesis. The experimental study of molecular recognition by
360 disordered proteins can be very challenging due to the rapid increase in complexity
361 inherent in multivalent binding. Competition, cooperativity and multiple binding
362 modes often limit the study to global behaviour only (in which mechanistic
363 information may be lost), or dissection into simpler pairwise interactions, treating
364 the intervening sequences as inert (which may incur the loss of important
365 information on e.g. cooperativity). SPR data on such systems is often high quality in
366 both signal-to-noise and reproducibility, while being deemed "unfittable" due to the
367 ill-posed problem of decomposing a distribution of exponentials. However we find
368 that the combination of regularization and Bayesian approaches (37), designed for
369 the deconvolution of mass transport and surface heterogeneity, is also very effective
370 at decomposing multivalent interactions. The resulting distributions may be
371 subsequently validated by competition and mutagenesis, as we have done here,
372 alongside mapping by NMR, which is both residue-specific and sensitive to a wide
373 range of interaction affinities (40).
374 In addition to the secondary sites and mini-SLiMs we establish in this study,
375 further evidence for weak, non-canonical engagement of Calcineurin with
376 hydrophobic residues is seen in the existing PxIxIT peptide/Calcineurin X-ray crystal
377 structures, in which the reverse face of the PxIxIT site provides an additional
378 potential encounter point (Supp. Fig. 6a). In the structures, one with PVIVIT (20) and
379 one with the AKAP sequence PIAIIIT (21), the stoichiometry in the asymmetric unit is
380 two Calcineurin heterodimers to one peptide, with the second heterodimer binding
381 to the opposite side of the PxIxIT site, out of register by one residue towards the C-
382 terminus of AKAP5. The peptide thus forms an axis of pseudosymmetry. In both
383 cases, the first heterodimer that engages the consensus elements of the PxIxIT
384 sequence has a larger buried surface area and a greater number of hydrogen bonds.
385 The opposite side displays VxV or AxI, to which a second heterodimer is bound in the

386 crystal, using the same hydrophobic PxIxIT-binding groove, but with significantly
387 lower affinity, since no evidence for a 2:1 stoichiometry was seen in solution by size
388 exclusion chromatography or SEC-MALS (20, 21). However, the presence of
389 hydrophobic residues in the two 'x' positions may serve as an additional capture
390 surface on PxIxIT, even if unstable. Their presence may (partially) account for the
391 fact that in our experiments, mutation of the three distal secondary sites in
392 AKAP5c$_{ILVF->SA}$ did not restore 'pure' pseudo first-order binding characteristic of
393 simple bimolecular collisions (Fig. 5b & e). Considered as a group, PxIxIT affinities
394 span a wide range, and the fine-tuning of PxIxIT affinities by altering the 'x' positions
395 presumably facilitates evolution into either anchoring or signalling roles. It is
396 interesting to note that during selection for competitive peptide inhibitors of PxIxIT
397 binding there was a clear enrichment for hydrophobic residues (V, I and L) in the two
398 x positions (41), while many of the low affinity substrates favour charged or polar
399 amino acids in these positions that would be incompatible with the non-polar groove
400 on Calcineurin e.g. PRIEIT in NFATc1 (25 µM; Supp. Fig. 6b).
401 Our findings also demonstrate that SLiM recognition in AKAP5c is non-
402 exclusive: both Calcineurin and Calmodulin recognise features of the canonical PKA
403 SLiM and therefore all three are in competition for the same site (Fig. 2 & 3).
404 Interactions of one SLiM with many partners have been documented (42), and due
405 to the substitution-tolerant nature of SLiMs coupled with the conformational
406 plasticity of IDPs, may be a common feature of disordered scaffolds. In this example,
407 PKA has a higher affinity for AKAP5c than Calcineurin (and presumably Calmodulin).
408 However, the *in vivo* concentration of cellular PKA is sub-µM (43) whereas
409 concentrations of Calcineurin are generally much higher (e.g. 1% of the total protein
410 concentration in brain (44)), and further concentrated at the membrane or
411 cytoskeletal elements (45). A slowly diffusing pool of highly concentrated Calcineurin
412 (or Calmodulin), fed by an intrinsically high cellular presence and maintained by
413 other local SLiMs, will have a high effective concentration and therefore be

414 competitive. Moreover, due to the high abundance of AKAPs, there is likely to be an
415 excess of anchoring sites compared to the kinase (46).
416 Parallels can be drawn between this 'labile but localised' pool of Calcineurin
417 that supplies the canonical anchoring site with the ways transcription factors (TFs)
418 bind DNA. TFs recognize their binding site with high affinity, but also bind, albeit with
419 low affinity, to non-canonical DNA and *via* mechanisms such as sliding, jumping and
420 monkey bar strand transfer reduce the dimensionality of the search (47, 48). The
421 recognition of IDPs containing multiple SLiMs of different affinities for a partner is
422 likely to share similar properties, for which the term 'allovalency' has been coined
423 (12, 49).
424 Here we uncover several Calcineurin interaction motifs spanning a range of
425 affinities from nM-mM in a short region of a scaffold protein. At least three
426 hydrophobic patches bind the Calcineurin PxIxIT groove with µM affinity, which is
427 similar to Calcineurin's affinity for many of its PxIxIT-containing substrates. The
428 patches in AKAP5c are conserved across relevant AKAPs (Supp. Fig. 1b) and do
429 indeed appear to bestow a biologically useful function: to enhance capture and
430 anchoring, while maintaining a more mobile pool of Calcineurin than would be
431 present if the anchoring protein contained one ultra-high affinity SLiM. The mM-
432 affinity partial/mini-SLiMs may act together to further conserve the hydrophobic
433 'capacitance' of the region responsible for Calcineurin capture.
434
435 **Conclusion**
436 The scaffolding protein AKAP5 contains a well-characterised PxIxIT-motif Calcineurin
437 binding site. We characterise at least three additional binding sites of lower affinity
438 C-terminal to the PxIxIT site and propose that these additional sites create a 'labile
439 but localised' pool that supplies Calcineurin to both the canonical anchoring site and
440 to downstream effectors such as NFAT. We conclude that in AKAP5, the disordered
441 regions between anchoring SLiMs, rather than being inert tethers, are enriched in

442 lower-affinity/mini-SLiMs that act together to maintain a stable but responsive
443 signalosome.
444
445 **Materials and Methods**
446 **Constructs**
447 pcDNA™3.1 V5-His TOPO containing full length human AKAP5 with V5 and His tags
448 was obtained. AKAP5c$_{ILVF->SA}$ was generated by gene synthesis (GeneArt;
449 ThermoFisher). pOP5T was created from pOP5TT (Hyvönen *et al*., unpublished), by
450 deletion of thioredoxin leaving a TEV-removable N-terminal octa-His tag. pET15b
451 CnA CnB, which contains human PPP3CA and PPP3R1 (50) was obtained from
452 Addgene (11787). Plasmid pQE30 CaM containing rat Calmodulin (protein sequence
453 100% identical to human) was obtained from Dermot Cooper, Department of
454 Pharmacology, University of Cambridge. NanoBiT vectors were obtained from
455 Promega.
456 Cloning was carried out using standard molecular biology techniques. The
457 coding sequence for AKAP5c was PCR amplified from pCDNA3.1 hAKAP and inserted
458 between the BamHI and HindIII sites of pHAT3 using restriction cloning. All other
459 cloning was carried out using a modified SLIC protocol based on (51). The
460 appropriate plasmid and insert sequences (see above) with 15 bp complementary
461 overhangs, or 12 bp for deletion of the PIAIIIT site were amplified using Q5
462 polymerase (NEB). For unique Cys mutants, a Cys codon was added to the forward
463 primer immediately after the GS in the Thrombin or TEV site. Final constructs were:
464

pHAT3 AKAP5c	Human AKAP5 300-427 with a Thrombin-cleavable His$_6$ tag
pHAT3 AKAP5c$_{\Delta PIAIIIT}$	Human AKAP5 300-427 Δ337-343 (PIAIIIT) with a Thrombin-cleavable His$_6$ tag
pOP5T AKAP5c$_{ILVF->SA}$	Human AKAP 300-427 F362A, L363S, I364A, L391A, L392S, I393A, L406S, I408A, L411S, V412A with a TEV cleavable N-terminal His$_8$ tag
pOP5T Cys-AKAP5c	Human AKAP 300-427 with a TEV cleavable N-terminal His$_8$ tag and an N-terminal Cys
pOP5T Cys-AKAP5c$_{\Delta PIAIIIT}$	Human AKAP 300-427 Δ337-343 (PIAIIIT) with a TEV cleavable N-terminal His$_8$ tag and an N-terminal Cys
pOP5T Cys-AKAP5c$_{ILVF->SA}$	Human AKAP 300-427 F362A, L363S, I364A, L391A, L392S, I393A, L406S, I408A, L411S, V412A with a TEV cleavable N-

	terminal His_8 tag and an N-terminal Cys
pOP5T CaM	Rat Calmodulin with a TEV cleavable N-terminal His_8 tag
pBiT1.1-C AKAP5	Full-length human AKAP5-LgBiT
pBiT2.1-C AKAP5	Full-length human AKAP5-SmlBiT
NanoBiT™ Negative Control Vector	HaloTag®-SmlBiT
LgBiT-PRKAR2A Control Vector	LgBiT-PRKAR2A (RIIA regulatory subunit of PKA)

465 Protein sequences are presented in full in Supplementary Information.

466

467 **Protein expression and purification**

468 All proteins were expressed in *E.coli* BL21(DE3) or BL21 Star (DE3) cells transformed
469 with the appropriate plasmid. For unlabelled proteins 2 L baffled flasks containing
470 500 ml of AIM LB or AIM 2YT autoinduction medium (Formedium) supplemented
471 with 50 µg/ml carbenicillin (and 1 mM $CaCl_2$ for Calmodulin) were inoculated with
472 1% starter culture in LB medium and grown overnight at 30 °C with shaking at 170
473 rpm. Labelled proteins were expressed similarly, but in M9 minimal medium
474 containing (as appropriate) 0.4 g/L ^{15}N ammonium chloride, 4g/L uniformly labelled
475 ^{13}C glucose as the sole nitrogen and carbon sources and supplemented with 5%
476 Celtone complete medium with the appropriate isotopic labelling. Cells were grown
477 to an OD_{600} of 0.7 before induction with 0.5 mM IPTG, and grown overnight at 23 °C.
478 AKAP and Calmodulin constructs expressed from either pHAT3 or pOP5T
479 were purified as follows: cells were resuspended in IMAC buffer A (20mM Tris pH
480 8.0, 0.5 M NaCl, 10 mM imidazole) with SIGMA*FAST* EDTA free protease inhibitor
481 cocktail. Cells were lysed using an Emulsiflex and clarified lysate was heated at 70 °C
482 for 20 min. Precipitated protein was removed by centrifugation and the supernatant
483 further purified by Ni-NTA affinity chromatography. Bound proteins were eluted with
484 IMAC buffer B (A containing 400 mM imidazole) and dialysed overnight into 20 mM
485 Tris pH 8.0 using 7 kDa cut-off membrane, the His tag was removed with thrombin
486 (pHAT3) or TEV (pOP5T), uncut protein removed by passing over Ni-NTA resin, and
487 proteins further purified using a 6 ml Resource Q column (Cytiva) eluted with a linear
488 NaCl gradient 0-400 mM. DTT (2 mM) was present in all steps after the initial Ni-NTA
489 purification of proteins containing a unique cysteine. Proteins were concentrated
490 and buffer exchanged into the appropriate buffer before storage at –80 °C.

491 Calcineurin was purified similarly, except that rather than heating, it was
492 precipitated from clarified lysate by addition of ammonium sulphate to 45%
493 saturation on ice before being resuspended in IMAC buffer A, and the His tag on the
494 A subunit was not removed. After elution from the Resource Q column, Calcineurin
495 was concentrated to ~ 5-10 mg/ml and further purified by size exclusion
496 chromatography using an S200 16/600 column (Cytiva) in 20 mM Tris/HCl pH 7.4,
497 150 mM NaCl, 2 mM DTT and stored at –80 °C.
498
499 **Peptides**
500 Peptides (EPIAIIITDTE and DDQYLAVPQH) were purchased from Biomatik and
501 dialysed extensively against the appropriate buffer before use.
502
503 **Biotin labelling**
504 Proteins were labelled using EZ-Link™ Maleimide-PEG2-Biotin (ThermoFisher) in 10
505 mM PIPES pH 6.5, 150 mM NaCl according to the manufacturer's instructions.
506
507 **Concentration measurements**
508 Protein and peptide concentrations were determined spectophotometrically using a
509 NanoDrop One^{C} instrument (ThermoFisher) at 205 nm for the AKAP constructs (due
510 to their low ε_{280}) and 280 nm for Calcineurin and Calmodulin. Extinction coefficients
511 were calculated using https://spin.niddk.nih.gov/clore/Software/A205.html based
512 on Anthis & Clore, 2013 (52).
513
514 **Nuclear Magnetic Resonance**
515 NMR measurements were made on ^{15}N- or ^{13}C,^{15}N-labelled proteins (~100 µM) in 10
516 mM PIPES pH 6.5, 150 mM NaCl (NMR buffer) and 10-15% $^{2}H_2O$. Experiments were
517 recorded at 25 °C on Bruker DRX600 or 800 spectrometers. Assignments were
518 obtained using a conventional triple-resonance approach (HNCA, HN(CO)CA, HNCO,
519 HNCACB, HN(CO)CACB) alongside TOCSY-^{15}N-HSQC, NOESY-^{15}N-HSQC and

520 HNN/HN(C)N experiments (53, 54). Data were processed using AZARA (v.2.7, ©
521 1993-2021; Wayne Boucher and Department of Biochemistry, University of
522 Cambridge). Triple resonance experiments were recorded with 25% nonuniform
523 sampling, using Poisson-gap sampling (55), and reconstructed using the Cambridge
524 CS package and the CS-IHT algorithm (56). Assignments were made using CcpNmr
525 Analysis v. 2.4 (57). Chemical shifts were referenced to 2,2-dimethyl-2-silapentane-5-
526 sulfonic acid (DSS). Heteronuclear NOE values were obtained at 600 MHz with either
527 4 s of ^{1}H saturation using a 120° pulse train or a 4 s delay prior to the first ^{15}N pulse
528 (58). Complexes with Calcineurin were first prepared at the defined stoichiometries
529 in 10 mM Tris/HCl pH 7.4, 150 mM NaCl, 2 mM DTT and then dialysed into NMR
530 buffer. Peptides were added from concentrated stocks to minimise dilution effects.
531 Intensity ratios were calculated using fitted peak heights in Analysis. Chemical-shift
532 differences were calculated using $\Delta\delta = [(\Delta\delta^{H})^2 + (0.15 \times \Delta\delta^{N})^2]^{1/2}$ (40).
533
534 **Far-UV Circular Dichroism Spectroscopy**
535 Experiments were performed at 0.1 mg/ml over a 185-260 nm range at 25 °C in 10
536 mM PIPES pH 6.5 and 150 mM NaF and in 1 mm path-length cuvettes. Spectra were
537 acquired using an AVIV 410 spectrometer in 1 nm wavelength steps, averaged over
538 three accumulations and baseline-corrected using buffer before smoothing, using
539 the manufacturer's software. Millidegree units were converted to mean residue
540 ellipticity (MRE) with units deg cm^{2} dmol^{-1} res^{-1} using MRE = millideg. / {(no. residues
541 – 1) × c × *l* × 10}, where c = molar concentration and *l* = path length in cm.
542
543 **Analytical Ultracentrifugation**
544 Sedimentation velocity was measured in an Optima XL-I centrifuge (Beckman
545 Coulter). For AKAP5c, standard 12 mm double-sector Epon centrepieces with
546 sapphire windows contained 400 µl of AKAP5c at 1 mg/mL or buffer (10 mM sodium
547 phosphate pH 6.5, 150 mM NaCl). Interference data were acquired at 40 krpm using
548 an An60 Ti four-hole rotor, at 20 °C. A multi-component sedimentation coefficient

549 *c*(*s*) distribution was obtained from 100 scans collected over 22 h by direct boundary
550 modelling of the Lamm equation using Sedfit v.15 (59). The density and viscosity of
551 the buffer (ρ = 1.0055 g/ml; η = 1.01881 cP) and the partial specific volume of the
552 protein (0.72918 ml/g) were calculated using Sednterp (60). For Calcineurin, 12 mm
553 double-sector Epon centrepieces with sapphire windows contained 400 µl of
554 Calcineurin at 0.4 mg/mL or buffer (10 mM PIPES pH 6.5, 150 mM NaCl, 5 mM DTT).
555 Interference data were acquired at 50 krpm using an An50 Ti eight-hole rotor, at 20
556 °C. A multi-component sedimentation coefficient *c*(*s*) distribution was obtained from
557 20 scans collected over 5 h by Sedfit, as above. The density and viscosity of the
558 buffer (ρ = 1.0054 g/ml; η = 1.02631 cP) and the partial specific volume of the
559 protein (0.73431 ml/g) were calculated by Sednterp, as above.
560
561 **Cell culture**
562 HEK293T cells were cultured in 10 cm tissue culture treated dishes grown at 37 °C in
563 a 5% CO_2 atmosphere in HEPES buffered DMEM/F12 1:1 (Merck) supplemented with
564 10% fetal bovine serum and 2 mM L-glutamine. Cells were maintained in logarithmic
565 growth phase and passaged upon reaching ~80% confluence (every 2-3 days).
566
567 **Split-Luciferase Reporter Assays (NanoBiT)**
568 Split luciferase reporter assays were carried out using the Promega NanoBiT system.
569 Briefly, cells were diluted in in HEPES buffered DMEM/F12 1:1 (Merck)
570 supplemented with 10% fetal bovine serum and 2 mM L-glutamine to 50,000
571 cells/ml and plated at a density of 5000 cells per well (100 µl) in 96-well white clear-
572 bottom tissue culture treated plates (Corning 3610). Cells were grown for 24 h
573 before transfection. Cells were transiently transfected with 50 ng each of the
574 appropriate plasmids using FuGENE HD (Promega) at a FuGENE DNA ratio of 3:1.
575 After transfection cells were grown for a further 24 h before assay.
576 Plates were left to equilibrate at room temperature for 20 minutes before addition
577 of NanoGlo live cell substrate (Promega) according to the manufacturer's

578 instructions. After mixing at 800 rpm for 10 s, luminescence was assayed in a
579 PHERAstar microplate reader (BMG LABTECH) at 25 °C using bottom optics and an
580 averaging time of 10 s.
581
582 **Surface Plasmon Resonance**
583 Experiments were performed on a Biacore T200 instrument (GE) at 25 °C. Biotin-Cys-
584 AKAP5c, Biotin-Cys-AKAP5c$_{ILVF->SA}$ and Biotin-Cys-AKAP5c$_{\Delta PIAIIIT}$ were immobilised on
585 separate channels of an SA sensor chip (Cytiva). In order to optimise the analyte
586 response signal-to-noise ratio, 12 RU were immobilised for AKAP5c and AKAP5c$_{ILVF-}$
587 $_{>SA}$, and 55 RU for AKAP5c$_{\Delta PIAIIIT}$; analyte responses for AKAP5c$_{\Delta PIAIIIT}$ were
588 subsequently re-scaled by a factor of 12/55 for comparative purposes. Binding to
589 AKAP5c and AKAP5c$_{ILVF->SA}$ was determined in 10 mM PIPES pH 6.5, 150 mM NaCl,
590 0.05% v/v Tween20, at ten Calcineurin concentrations (0, 10, 20, 40, 80, 160, 320,
591 640, 1280 and 2560 nM). Binding to AKAP5c$_{\Delta PIAIIIT}$ was determined at nine
592 Calcineurin concentrations (0, 78, 156, 313, 625, 1250, 2500, 5000 and 10000 nM).
593 All concentrations were run in duplicate. The contact time, dissociation time and
594 flow rate were 300 s, 1200 s and 30 µL min^{-1}, respectively. The chip surface was
595 regenerated with 50 mM NaOH, 1 M NaCl for 1 or 2 x 60 s. Data were processed
596 using the manufacturer's BIAevaluation software and further analysis was carried
597 out in EVILFIT (37).
598
599 **Data availability**
600 Chemical-shift assignments for AKAP5c (see also Supp. Fig. S2) have been deposited
601 in the BMRB with accession number XXXX.
602
603 **Acknowledgements**
604 We thank Peter Schuck, Marko Hyvönen and Anna Git for helpful discussions, the
605 NMR and Biophysics Facilities in the Department of Biochemistry, University of
606 Cambridge for access to instrumentation, and Dermot Cooper for the Calmodulin

607 plasmid. This work was supported by the Biotechnology and Biological Sciences
608 Research Council (BB/N022181/1).

609

610 **References**

611 1. Scott JD, Pawson T (2009) Cell signaling in space and time: Where proteins
612 come together and when they're apart. *Science* 326(5957):1220–1224.
613 2. Pan CQ, Sudol M, Sheetz M, Low BC (2012) Modularity and functional
614 plasticity of scaffold proteins as p(l)acemakers in cell signaling. *Cell Signal*
615 24(11):2143–2165.
616 3. Theurkauf WE, Vallee RB (1982) Molecular characterization of the cAMP-
617 dependent protein kinase bound to microtubule-associated protein 2. *J Biol*
618 *Chem* 257(6):3284–3290.
619 4. Lohmann SM, DeCamilli P, Einig I, Walter U (1984) High-affinity binding of the
620 regulatory subunit (R(II)) of cAMP-dependent protein kinase to microtubule-
621 associated and other cellular proteins. *Proc Natl Acad Sci U S A* 81(21 I):6723–
622 6727.
623 5. Wong W, Scott JD (2004) AKAP signalling complexes: Focal points in space and
624 time. *Nat Rev Mol Cell Biol* 5(12):959–970.
625 6. Torres-Quesada O, Mayrhofer JE, Stefan E (2017) The many faces of
626 compartmentalized PKA signalosomes. *Cell Signal* 37(May):1–11.
627 7. Davey NE, et al. (2012) Attributes of short linear motifs. *Mol Biosyst* 8(1):268–
628 281.
629 8. Roey K Van, et al. (2014) Short linear motifs: ubiquitous and functionally
630 diverse protein interaction modules directing cell regulation. *Chem Rev*
631 114:6733–6778.
632 9. Charlotte SS, Jendroszek A, Kjaergaard M (2019) Linker dependence of avidity
633 in multivalent interactions between disordered proteins. *J Mol Biol* 431:4784–
634 4795.
635 10. Bugge K, et al. (2020) Interactions by disorder – a matter of context. *Front Mol*
636 *Biosci* 7(June):1–16.
637 11. Liu BA, et al. (2010) SH2 domains recognize contextual peptide sequence
638 information to determine selectivity. *Mol Cell Proteomics* 9(11):2391–2404.
639 12. Klein P, Pawson T, Tyers M (2003) Mathematical modeling suggests
640 cooperative interactions between a disordered polyvalent ligand and a single
641 receptor site. *Curr Biol* 13:1669–1678.
642 13. Tompa P, Fuxreiter M (2008) Fuzzy complexes: polymorphism and structural
643 disorder in protein-protein interactions. *Trends Biochem Sci* 33(1):2–8.
644 14. Creamer TP (2020) Calcineurin. *Cell Commun Signal* 18(137):1–12.
645 15. Li H, Rao A, Hogan PG (2011) Interaction of calcineurin with substrates and
646 targeting proteins. *Trends Cell Biol* 21(2):91–103.
647 16. Donella-Deana A, Krinks MH, Ruzzene M, Klee C, Pinna LA (1994)
648 Dephosphorylation of phosphopeptides by calcineurin (protein phosphatase
649 2B). *Eur J Biochem* 219(1–2):109–117.
650 17. Li X, Wilmanns M, Thornton J, Köhn M (2013) Elucidating human phosphatase-
651 substrate networks. *Sci Signal* 6(275):1–15.

652 18. Aramburu J, et al. (1998) Selective inhibition of NFAT activation by a peptide
653 spanning the calcineurin targeting site of NFAT. *Mol Cell* 1:627–637.
654 19. Garcia-Cozar FJ, et al. (1998) Two-site interaction of nuclear factor of activated
655 T cells with activated calcineurin. *J Biol Chem* 273(37):23877–23883.
656 20. Li H, Zhang L, Rao A, Harrison SC, Hogan PG (2007) Structure of Calcineurin in
657 Complex with PVIVIT Peptide: Portrait of a Low-affinity Signalling Interaction. *J*
658 *Mol Biol* 369(5):1296–1306.
659 21. Li H, et al. (2012) Balanced interactions of calcineurin with AKAP79 regulate
660 Ca2+-calcineurin-NFAT signaling. *Nat Struct Mol Biol* 19(3):337–345.
661 22. Dell'Acqua ML, Dodge KL, Tavalin SJ, Scott JD (2002) Mapping the protein
662 phosphatase-2B anchoring site on AKAP79. Binding and inhibition of
663 phosphatase activity are mediated by residues 315-360. *J Biol Chem*
664 277(50):48796–48802.
665 23. Oliveria SF, Dell'Acqua ML, Sather WA (2007) AKAP79/150 anchoring of
666 calcineurin controls neuronal L-Type Ca2+ channel activity and nuclear
667 signaling. *Neuron* 55(2):261–275.
668 24. Newlon MG, et al. (2001) A novel mechanism of PKA anchoring revealed by
669 solution structures of anchoring complexes. *EMBO J* 20(7):1651–1662.
670 25. Btesh J, Fischer MJ, Stott K, McNaughton PA (2013) Mapping the binding site
671 of TRPV1 on AKAP79: implications for inflammatory hyperalgesia. *J Neurosci*
672 33(21):9184–9193.
673 26. Mack K, Fischer MJM (2017) Disrupting sensitization of TRPV4. *Neuroscience*
674 352:1–8.
675 27. Zhang X, Li L, McNaughton PA (2008) Proinflammatory mediators modulate
676 the heat-activated ion channel TRPV1 via the scaffolding protein AKAP79/150.
677 *Neuron* 59(3):450–461.
678 28. Dunker AK, et al. (2013) What's in a name? Why these proteins are
679 intrinsically disordered. *Intrinsically Disord Proteins* 1(e24157):1–5.
680 29. Marsh JA, Singh VK, Jia Z, Forman-Kay JD (2006) Sensitivity of secondary
681 structure propensities to sequence differences between α- and γ-synuclein:
682 Implications for fibrillation. *Protein Sci* 15(12):2795–2804.
683 30. Gold MG, et al. (2011) Architecture and dynamics of an A-kinase anchoring
684 protein 79 (AKAP79) signaling complex. *Proc Natl Acad Sci U S A*
685 108(16):6426–6431.
686 31. Patel N, Stengel F, Aebersold R, Gold MG (2017) Molecular basis of AKAP79
687 regulation by calmodulin. *Nat Commun* 8(1). doi:10.1038/s41467-017-01715-
688 w.
689 32. Nygren PJ, et al. (2017) Intrinsic disorder within AKAP79 fine-tunes anchored
690 phosphatase activity toward substrates and drug sensitivity. *Elife* 6:1–25.
691 33. Liao M, Cao E, Julius D, Cheng Y (2013) Structure of the TRPV1 ion channel
692 determined by electron cryo-microscopy. *Nature* 504(7478):107–12.
693 34. Rumi-Masante J, et al. (2012) Structural basis for activation of calcineurin by
694 calmodulin. *J Mol Biol* 415(2):307–317.
695 35. Sheftic SR, Page R, Peti W (2016) Investigating the human Calcineurin
696 Interaction Network using the πϕLxVP SLiM. *Sci Rep* 6(December):1–11.
697 36. Tidow H, Nissen P (2013) Structural diversity of calmodulin binding to its
698 target sites. *FEBS J* 280(21):5551–5565.

699 37. Schuck P, Zhao H (2010) The role of mass transport limitation and surface
700 heterogeneity in the biophysical characterization of macromolecular binding
701 processes by SPR biosensing. *Methods Mol Biol* 627:15–54.
702 38. Lagerholm BC, Thompson NL (1998) Theory for ligand rebinding at cell
703 membrane surfaces. *Biophys J* 74(3):1215–1228.
704 39. Gopich I V., Szabo A (2019) Diffusion-induced competitive two-site binding. *J*
705 *Chem Phys* 150(9). doi:10.1063/1.5079748.
706 40. Zuiderweg E (2002) Mapping protein–protein interactions in solution by NMR
707 spectroscopy. *Biochemistry* 41(1). Available at:
708 http://pubs.acs.org/doi/abs/10.1021/bi011870b [Accessed August 1, 2013].
709 41. Aramburu J, et al. (1999) Affinity-driven peptide selection of an NFAT inhibitor
710 more selective than cyclosporin A. *Science* 285(5436):2129–2133.
711 42. Hsu WL, et al. (2013) Exploring the binding diversity of intrinsically disordered
712 proteins involved in one-to-many binding. *Protein Sci* 22(3):258–273.
713 43. Beavo JA, Bechtel PJ, Krebs EG (1974) Activation of protein kinase by
714 physiological concentrations of cyclic AMP. *Proc Natl Acad Sci U S A*
715 71(9):3580–3583.
716 44. Yakel JL (1997) Calcineurin regulation of synaptic function: From ion channels
717 to transmitter release and gene transcription. *Trends Pharmacol Sci*
718 18(4):124–134.
719 45. Shibasaki F, Hallin U, Uchino H (2002) Calcineurin as a multifunctional
720 regulator. *J Biochem* 131(1):1–15.
721 46. Omar MH, Scott JD (2020) AKAP signaling islands: venues for precision
722 pharmacology. *Trends Pharmacol Sci* 41(12):933–946.
723 47. Gowers DM, Halford SE (2003) Protein motion from non-specific to specific
724 DNA by three-dimensional routes aided by supercoiling. *EMBO J* 22(6):1410–
725 1418.
726 48. Vuzman D, Azia A, Levy Y (2010) Searching DNA via a “monkey bar”
727 mechanism: the significance of disordered tails. *J Mol Biol* 396(3):674–684.
728 49. Levchenko A (2003) Allovalency: a case of molecular entanglement. *Curr Biol*
729 13(22):876–878.
730 50. Mondragon A, et al. (1997) Overexpression and purification of human
731 calcineurin α from Escherichia coli and assessment of catalytic functions of
732 residues surrounding the binuclear metal center. *Biochemistry* 36(16):4934–
733 4942.
734 51. Jeong JY, et al. (2012) One-step sequence-and ligation-independent cloning as
735 a rapid and versatile cloning method for functional genomics Studies. *Appl*
736 *Environ Microbiol* 78(15):5440–5443.
737 52. Anthis NJ, Clore GM (2013) Sequence-specific determination of protein and
738 peptide concentrations by absorbance at 205 nm. *Protein Sci* 22(6):851–858.
739 53. Cavanagh J, Skelton NJ, Fairbrother WJ, Rance M, Palmer AGI (2006) *Protein*
740 *NMR Spectroscopy Principles and Practice* (Academic Press). 2nd Ed.
741 54. Panchal SC, Bhavesh NS, Hosur R V (2001) Improved 3D triple resonance
742 experiments , HNN and HN(C)N, for HN and 15N sequential correlations in
743 (13C,15N) labeled proteins : Application to unfolded proteins. *J Biomol NMR*
744 20(C):135–147.
745 55. Hyberts SG, Takeuchi K, Wagner G (2010) Poisson-gap sampling and forward

746 maximum entropy reconstruction for enhancing the resolution and sensitivity
747 of protein NMR data. *J Am Chem Soc* 132(7):2145–2147.
748 56. Bostock MJ, Holland DJ, Nietlispach D (2012) Compressed sensing
749 reconstruction of undersampled 3D NOESY spectra: Application to large
750 membrane proteins. *J Biomol NMR* 54(1):15–32.
751 57. Vranken WF, et al. (2005) The CCPN data model for NMR spectroscopy:
752 Development of a software pipeline. *Proteins Struct Funct Genet* 59(4):687–
753 696.
754 58. Farrow NA, et al. (1994) Backbone dynamics of a free and a phosphopeptide-
755 complexed Src homology 2 domain studied by ^{15}N NMR relaxation.
756 *Biochemistry* 33(19):5984–6003.
757 59. Schuck P (2000) Size-distribution analysis of macromolecules by
758 sedimentation velocity ultracentrifugation and Lamm equation modeling.
759 *Biophys J* 78(3):1606–1619.
760 60. Laue TM, Shah BD, Ridgeway TM, Pelletier SL (1992) Computer-aided
761 interpretation of analytical sedimentation data for proteins. *Anal*
762 *ultracentrifugation Biochem Polym Sci* (October 2017):90–125.
763
764